Compound Kushen injection attenuates angiotensin II-mediated heart failure by inhibiting the PI3K/Akt pathway

WEI WANG[1*], DA LIU[1*], LIYUN YANG[2], LIXIA CHEN[1], MENGDAN MIAO[1], YONGSHENG LIU[1], YAJUAN YIN[1], MEI WEI[1], GANG LIU[1], YONGHUI AN[3] and MINGQI ZHENG[1,4]

[1]Department of Cardiology, The First Hospital of Hebei Medical University, Shijiazhuang, Hebei 050031; [2]Department of Biochemistry and Molecular Biology, Hebei Medical University, Shijiazhuang, Hebei 050017; [3]Department of Oncology, The First Hospital of Hebei Medical University, Shijiazhuang, Hebei 050031; [4]Hebei Key Laboratory of Heart and Metabolism, Shijiazhuang, Hebei 050000, P.R. China

Received November 3, 2022; Accepted January 19, 2023

DOI: 10.3892/ijmm.2023.5226

Abstract. Compound Kushen injection (CKI) is a type of traditional Chinese medicine that has previously been studied for the treatment of various types of cancer. Previous studies have reported that CKI regulates cell apoptosis by down-regulating the PI3K/Akt pathway. The present study aimed to determine whether CKI alleviates heart failure (HF) by attenuating cardiomyocyte apoptosis via the inhibition of the PI3K/Akt pathway. Angiotensin II (Ang II) was used to elicit HF, and osmotic minipumps with either Ang II (2 μg/kg/day) or phosphate-buffered saline (PBS; 200 μl) were subcutaneously implanted into 6-week-old male C57BL/6 mice for 3 weeks. In addition, PBS or CKI (25 mg/kg/day) were subcutaneously infused once a day for 3 weeks. Echocardiography was used to examine hemodynamics. The myocardial injury biomarkers, cardiac troponin I and N-terminal (NT)-pro hormone B-type natriuretic peptide, were assessed using enzyme-linked immunosorbent assay. Transmission electron microscopy was used to determine the morphology of the myocardium. The rate of apoptosis was detected using TUNEL staining and flow cytometry (FCM), and the expression levels of apoptosis-related proteins were measured using western blot (WB) analysis. Moreover, H9C2 cells were treated with CKI (2 mg/ml) or LY294002 (an inhibitor of the PI3K/Akt pathway; 25 μmol/l) in combination with Ang II (1 μmol/l) for 48 h. Cell Counting Kit-8 assay, FCM and WB analysis were performed in the H9C2 cells to examine cell viability, cell cycle distribution and representative signaling proteins. It was found that CKI promoted healthy cardiac function, reduced myocardial structural damage and reduced the rate of cardiomyocyte apoptosis. CKI markedly attenuated the expression of apoptosis-related proteins in the PI3K/Akt pathway. The results of the *in vitro* experiments indicated that CKI promoted cardiomyocyte proliferation and inhibited apoptosis, similar to LY294002. On the whole, the present study demonstrates that CKI reduces cardiomyocyte apoptosis, promotes healthy cardiac function and attenuates Ang II-mediated HF. These ameliorative effects may be associated with the inhibition of the PI3K/Akt pathway.

Correspondence to: Professor Mingqi Zheng, Department of Cardiology, The First Hospital of Hebei Medical University, 89 Donggang Road, Yuhua, Shijiazhuang, Hebei 050031, P.R. China
E-mail: mzheng@hebmu.edu.cn

Professor Yonghui An, Department of Oncology, The First Hospital of Hebei Medical University, 89 Donggang Road, Yuhua, Shijiazhuang, Hebei 050031, P.R. China
E-mail: sjzyhd@vip.sina.com

*Contributed equally

Abbreviations: HF, heart failure; Ang II, angiotensin II; CKI, compound Kushen injection; TCM, traditional Chinese medicine; PBS, phosphate-buffered saline; ELISA, enzyme-linked immunosorbent assay; DAPI, 4',6'-diamidino-2-phenylindole; PI, propidium iodide; FBS, fetal bovine serum; CCK-8, Cell Counting Kit-8; t-Akt, total Akt; p-Akt, phosphorylated Akt; cyto *c*, cytochrome *c*; LVDS, left ventricular end-systolic diameter; LVDD, left ventricular end-diastolic diameter; LVFS, left ventricular fraction shortening; LVEF, left ventricular ejection fraction; cTn I, cardiac troponin I; FCM, flow cytometry; WB analysis, western blot analysis; TEM, transmission electron microscopy

Key words: heart failure, PI3K/Akt pathway, apoptosis, CKI, cardiac function, LY294002

Introduction

Heart failure (HF) is a complex clinical syndrome that is induced by the functional impairment of ventricular systolic or diastolic functions (1). Worldwide, >1 million patients are hospitalized annually due to HF (2), and ~40% of these patients are re-hospitalized or succumb to the condition within ~1 year following diagnosis (3). The pathophysiological mechanisms of HF involve a variety of factors, including cardiomyocyte apoptosis, oxidative stress, calcium overload, inflammation and mitochondrial dysfunction. Notably, cardiomyocyte apoptosis remains the main cause of HF (4). Increased cardiomyocyte apoptosis is observed in both patients with end-stage HF and in experimental rats with HF (5). As HF exerts a negative

effect on morbidity and mortality, successful treatment options are required to improve patient survival rates and quality of life (6).

Previous research has indicated that elevation of angiotensin II (Ang II) levels is present in patients with HF, which highlights that Ang II stimulation is associated with HF (7). The results of a previous study demonstrated that rats treated with Ang II exhibited decreased cardiac systolic and diastolic function, accompanied by notable cardiomyocyte apoptosis in myocardial tissue (8). Therefore, Ang II is often used for the establishment of models of HF (9). Cardiac apoptosis is involved in the decline of cardiac function induced by Ang II (10). An increase in the levels of Ang II may trigger the activation of the PI3K/Akt signaling pathway to induce apoptosis (11). Thus, in the present study, Ang II was used to mimic cardiomyocyte apoptosis in a model of HF.

Compound Kushen injection (CKI) is a type of traditional Chinese medicine (TCM) that is extracted from Kushen (*Radix Sophorae Flavescentis*) and Tufuling *(Rhizoma Smilacis Chinae)* (12,13). The active compounds of CKI consist of matrine, oxymatrine, sophocarpine, sophoridine and kurarinone. The results of a previous study demonstrated numerous pharmacological properties of CKI, including antitumor, analgesic, immunity-enhancing and anti-inflammatory activities (14). CKI is extensively used in the treatment of numerous malignancies, including breast, lung and liver cancer (15). CKI is often used alone, or in combination with chemotherapy or radiotherapy (16). Notably, the results of a previous study demonstrated that CKI regulated cell proliferation via tge downregulation of the PI3K/Akt/mTOR pathway (17). The PI3K family is involved in a number of signaling pathways, and it regulates cell proliferation, differentiation, survival and apoptosis (18). The PI3K/Akt pathway is the main signaling pathway involved in cardiomyocyte apoptosis (19). An increased expression of PI3K leads to cardiomyocyte apoptosis and ultimately results in impaired ventricular systolic and diastolic function. The inhibition of the PI3K/Akt pathway may exert protective effects against HF (20). Thus, it was hypothesized that CKI may attenuate cardiomyocyte apoptosis and exert protective effects on heart function via the inhibition of the PI3K/Akt pathway.

Matrine and oxymatrine are the major active components of CKI. The cardioprotective effects of matrine and oxymatrine have been previously reported (21,22). Matrine can decrease myocardial stiffness and ameliorate myocardial compliance, and contributes to improving cardiac function (23). Cardiovascular injury is attenuated by matrine through the regulation of the PI3K/Akt pathway (24). Matrine ameliorates apoptosis in Ang II-mediated HF via the regulation of Bcl-2/Bax expression and caspase-3 activation (25). Additionally, previous research has reported that oxymatrine pre-treatment protects cardiomyocytes from cell damage, cell apoptosis and oxidative stress induced by hypoxia/reoxygenation by modulating the PI3K/Akt pathway (26).

As CKI is a combination of matrine, oxymatrine, sophocarpine, sophoridine and kurarinone, it remains unclear as to whether CKI protects against HF by attenuating PI3K/Akt-induced apoptosis. The present study thus aimed to evaluate these mechanisms through the establishment of an Ang II-mediated HF model *in vivo* and *in vitro*.

Materials and methods

Materials, reagents and antibodies. Human Ang II (24738) and phosphate-buffered saline (PBS; 600221) was obtained from Cayman Chemical Company. CKI with a total alkaloid concentration of 26.5 mg/ml in a 5-ml ampoule was obtained from Shanxi Zhendong Pharmaceutical Co. Ltd. Commercial enzyme-linked immunosorbent assay (ELISA) kits for cardiac troponin I (cTn I; E08421m) and N-terminal (NT)-pro hormone B-type natriuretic peptide (NT-proBNP; E05153m) were purchased from Cusabio Technology, LLC. The Epon812 resin (02334), dodecenylsuccinic anhydride (00563), dimethylaminomethyl phenol (17806), methyl nadic anhydride (00886), uranyl acetate (21447) and lead citrate (25350) were purchased from Polysciences, Inc. The TUNEL *In Situ* Cell Death Detection kit was purchased from the Beyotime Institute of Biotechnology. The 4',6'-diamidino-2-phenylindole (DAPI) was purchased from AAT Bioquest, Inc. The 1X binding buffer, Annexin V-PE, 7-AAD and propidium iodide (PI) were purchased from BD Biosciences. Trypsin-EDTA solution, DMEM, penicillin and streptomycin were obtained from Gibco; Thermo Fisher Scientific, Inc. Fetal bovine serum (FBS) was purchased from Shanghai ExCell Biology, Inc. The Cell Counting Kit-8 (CCK-8) was purchased from Dojindo Laboratories, Inc. The BCA protein quantification kit was purchased from Vazyme Biotech Co., Ltd. The BioTrace NT nitrocellulose membrane (66487) was purchased from Pall Life Sciences. Skim milk (abs9175) was obtained from Absin Bioscience Inc. The chemiluminescence detection kit (BL520A) was obtained from Biosharp Life Sciences. Primary antibodies against total Akt (t-Akt) (cat. no. GB111114), Bax (cat. no. GB11690) and Bcl-2 (cat. no. GB112382) were purchased from Wuhan Servicebio Technology Co., Ltd. Phosphorylated Akt (p-Akt) (cat. no. 66444-1-lg) and GAPDH (cat. no. BC004109) antibodies were purchased from Proteintech Group, Inc. Primary antibodies against cleaved caspase-3 (cat. no. 9661) and cleaved caspase-9 (cat. no. 9507) were purchased from Cell Signaling Technology, Inc. Primary antibodies against cytochrome *c* (cyto *c*) (cat. no. Ab-AF0146), p27 (cat. no. Ab-AF6324) and cyclin D1 (cat. no. Ab-AF0931) were purchased from Affinity Biosciences. Goat anti-rabbit IgG (cat. no. A23920) and goat anti-mouse IgG (cat. no. A23710) were obtained from Abbkine Scientific Co., Ltd. Primary antibodies against PI3K (cat. no. ab191606), goat anti-mouse IgG H&L (Alexa Fluor®647, cat. no. ab150115) and goat anti-rabbit IgG H&L (Alexa Fluor®647, cat. no. ab150077) were provided by Abcam. LY294002 (cat. no. 440202) and RIPA buffer (cat. no. 42029053) was acquired from MilliporeSigma.

Osmotic minipumps were purchased from Durect Corporation (Alzet Model 2004). The M-mode echocardiograph imaging system was purchased from FUJIFILM VisualSonics (Vevo 2100 system). A transmission electron microscope was purchased from Hitachi, Ltd. TUNEL analysis software was obtained from Image Pro-Plus software (Media Cybernetics, Inc.). An Olympus Fluoview FV1000 microscope was purchased from Olympus Corporation. A microplate reader was obtained from PerkinElmer, Inc. A FC-500 type flow cytometer and EXPO 32 ADC software (version no. 1.2) were obtained from Beckman Coulter, Inc. Multicycle AV

software was purchased from Phoenix Pharmaceuticals, Inc. (version no. 275).

Animals. All animal procedures were performed in accordance with the Guide for the Care and Use of Laboratory Animals published by the US National Institutes of Health (27), and all animal experiments were approved by the Institutional Animal Care and Use Committee of The First Hospital of Hebei Medical University, Shijiazhuang, China (ethics approval no. 20220634; date of approval: June 10, 2022).

Male C57BL/6 mice (age, 6 weeks; weight, 20-22 g) were purchased from Skbex Biotechnology, housed in cages with a 12/12-h light/dark cycle and provided with free access to water and food at 24˚C and a relative humidity of 50-70%. The mice were randomly divided into the following four groups: i) The control group (CON group, n=10); ii) the CKI group (n=10); iii) the Ang II group (Ang II group, n=10); and iv) the Ang II plus CKI group (AC group, n=10).

All mice were anesthetized with an intraperitoneal injection of pentobarbital sodium (40 mg/kg) prior to surgery. Subsequently, the mice in the Ang II and AC groups were treated with Ang II (2 μg/kg/min) through osmotic minipumps for 3 weeks, as previously described (28). The minipump was subcutaneously implanted into the back of each mouse for 21 days. In addition, mice in the CON and CKI groups were subcutaneously implanted with osmotic minipumps containing 200 μl PBS.

Zhao *et al* (29) reported that CKI treatment was maximally effective at concentrations of ≥25 mg/kg/day. Thus, in the present study, CKI was administered at 25 mg/kg/day. The mice were intraperitoneally injected with CKI once a day for 3 weeks in the CKI and AC groups, and mice in the CON and Ang II groups were injected with an equal volume of PBS at the same time intervals. In the present study, each experiment was carried out three times.

Hemodynamics and echocardiography. The mice were anesthetized with an intraperitoneal injection of pentobarbital sodium (40 mg/kg) following 3 weeks of treatment. Subsequently, M-mode echocardiography was carried out using a 30-MHz probe. Changes in left ventricular end-systolic diameter (LVDS), left ventricular end-diastolic diameter (LVDD), left ventricular ejection fraction (LVEF) and left ventricular fraction shortening (LVFS) were determined.

ELISA. Following M-mode echocardiography, when the mice were still anesthetized with pentobarbital sodium, a glass capillary was used to collect blood from the inner canthus of the mice. The blood samples were centrifuged at 1,100 x g for 5 min at room temperature, the separated sera were used to determine the serum concentrations of cTn I and NT-proBNP. The concentrations were measured using commercial ELISA kits, as aforementioned. The absorbance was recorded at 450 nm using a Multiskan® 96-well plate reader.

Morphometric analysis. At the end of the monitoring period, 40 mice were sacrificed via spinal cord dislocation. The heart tissues were removed, and five samples from each group were used for morphometric analyses, flow cytometry (FCM) and western blot (WB) analysis. The left ventricle of the heart was removed for transmission electron microscopy (TEM). For TEM, the tissues were prefixed with 2.5% glutaraldehyde in 0.1 M PBS pH 7.2 for 24 h at 4˚C. The samples were then washed twice with 0.1 M PBS and post-fixed for 1 h with 1% osmium tetroxide in 0.1 M PBS at 4˚C. The samples were respectively dehydrated according to the gradient of 50, 70, 90 and 100% dehydrated acetone and the dehydration was performed for 10 min with each concentration of dehydrated acetone three times. The dehydrated samples were then treated at 37˚C for 24 h in a mixture of epoxy resin and pure acetone (1:1), followed by 24 h of embedding at 60˚C in a mixture of Epon812 resin, dodecenylsuccinic anhydride, dimethylaminomethyl phenol and methyl nadic anhydride (26:6:1:19). The tissues were then cut into ultrathin slices (70 nm), followed by double staining with uranyl acetate (30 min) and lead citrate (10 min) at room temperature. The observation of ultrastructural alterations in the myocardial sections was performed using a transmission electron microscope.

FCM assay. Left ventricular tissue was removed as described above. The tissues were washed with ice-cold PBS and cut into sections of 1-mm^3. Subsequently, an enzyme solution (0.1% trypsin and 0.02% EDTA) was added, and the samples were maintained in a 37˚C water bath or thermostat shaker for digestion for 20-60 min. Digestion was terminated following the addition of serum-containing medium. Cell suspensions were collected in batches and filtered through a 100-mesh filter, followed by centrifugation at 2,000 x g for 5 min at 4˚C. Subsequently, the supernatant was discarded. The cells were washed with ice-cold PBS and centrifuged at 2,000 x g for 5 min at 4˚C, and 1-ml single-cell suspension was collected from each group. The cells were washed with ice-cold PBS and suspended in 100 μl 1X binding buffer. Subsequently, 5 μl Annexin V-PE were added, and the mixture was placed on ice for 15 min in the dark. A total of 400 μl 1X binding buffer and 5 μl 7-AAD were subsequently added. Following incubation on ice for 15 min in the dark at room temperature, the cells were washed once with ice-cold PBS, resuspended in 1 ml PBS and analyzed using an FC-500 flow cytometer. The apoptotic rate was measured using EXPO 32 ADC software (version no. 1.2).

TUNEL assay. The remaining five heart tissues from each group were fixed in 4% paraformaldehyde (in PBS, pH 7.4) for 30 min at room temperature, embedded in paraffin and cut into 5-mm-thick serial sections for TUNEL staining to evaluate cardiomyocyte apoptosis. TUNEL detection solution was added and sections were incubated the dark at 37˚C for 2 h. Nuclear staining was conducted using 1 μg/ml DAPI in PBS for 15 min at room temperature. The stained samples were analyzed using an Olympus Fluoview FV1000 microscope, and cells from 10 visual fields were randomly selected to determine the apoptotic index. The *In Situ* Cell Death Detection kit was used to analyze cardiomyocyte apoptosis. The digitally captured images of immunofluorescence in five randomly selected fields from each sample were analyzed using analysis software. The percentage of apoptotic cells was measured and recorded as the apoptotic index (AI%).

Cell culture and cell viability assay. The H9C2 cell line (cat. no. 1101RAT-PUMC000219) was purchased from the China Infrastructure of Cell Line Resources (Institute of Basic

Medical Sciences, Chinese Academy of Medical Sciences). The cells were cultured in DMEM supplemented with 10% FBS, penicillin (100 U/ml) and streptomycin (100 mg/ml) in a 37˚C humidified atmosphere containing 5% CO_2 and 95% O_2. Ang II (1 μmol/l) was used to mimic HF *in vitro*, as previously described (10). For all the *in vitro* experiments performed in the present study, CKI was used at a dilution of a final concentration of 2 mg/ml total alkaloids (30). LY294002 (25 μmol/l) was used as a PI3K/Akt pathway inhibitor, as previously reported (31). The H9C2 cells ($3x10^4$ cells/ml) were seeded in a 96-well plate and subsequently divided into four groups for incubation for 48 h at 37˚C as follows: The CON group was treated with medium (50 μl), the Ang II group was treated with Ang II (50 μl), the AC group was treated with Ang II (50 μl) + CKI (50 μl), and the AL group was treated with Ang II (50 μl) and the PI3K/Akt pathway inhibitor, LY294002 (50 μl).

CCK-8 assay was used to detect cell viability. A total of 10 μl of the CCK-8 solution was added to each well and incubated for 2 h at 37˚C, and the optical density was measured at 450 nm using a microplate reader.

Cell cycle distribution analysis. The effect of CKI on cell cycle distribution was analyzed using FCM with PI staining. Briefly, a total of 1 ml of single-cell suspension was collected from each group following the aforementioned treatments. The H9C2 cells were washed with ice-cold PBS and fixed with 70% alcohol at 4˚C for 24 h. Following washing twice with ice-cold PBS, the cells were suspended in 100 μl PBS, and 1 ml PI was added to the suspension for staining at 4˚C for 30 min, prior to cell cycle detection using an FC-500 type flow cytometer. Data were analyzed using Multicycle AV software.

WB analysis. Protein was extracted from left ventricular tissue or H9C2 cells for WB analysis. The tissues or cells were lysed using RIPA buffer (50 mM Tris-HCl; pH 7.4; 150 mM NaCl; 1% Triton X-100; 1% sodium deoxycholate). Protein concentrations was determined by BCA assay. Equal amounts of protein (20 μg) were separated with 6-15% SDS-PAGE gel and transferred onto a BioTrace NT nitrocellulose membrane and incubated with 5% skimmed milk for 1 h at room temperature. Subsequently, the membrane was incubated with the primary antibodies overnight at 4˚C. The reaction was then performed using a secondary antibody matching the primary antibody for 1 h at room temperature. The primary antibodies employed for WB were against PI3K (1:1,000), p-Akt (1:5,000), t-Akt (1:1,000), Bax (1:1,000), Bcl-2 (1:1,000), cyto *c* (1:500), cleaved caspase-9 (1:1,000), cleaved caspase-3 (1:1,000), p27 (1:500), cyclin D1 (1:500) and GAPDH (1:20,000). Secondary antibodies were all diluted at 1:2,000. The target proteins in the membranes were visualized using an enhanced chemiluminescence detection kit with an Odyssey Imaging System (Odyssey; version no. 3.0). Protein bands were quantified using ImageJ (National Institutes of Health) software (version 1.8.0) for densitometric analysis and normalized to GAPDH.

Statistical analysis. All data are presented as the mean ± standard error of the mean (M ± SEM). The results were analyzed using GraphPad Prism (version 8.0; GraphPad Software, Inc.). Depending on the design of the experiment, the data were analyzed using one-way ANOVA followed by Tukey's post hoc test. $P<0.05$ was considered to indicate a statistically significant difference.

Results

CKI improves cardiac compliance. Heart functions were evaluated using Doppler M-mode ultrasonography, as illustrated in Fig. 1A. The results demonstrated that the LVEF values were notably higher in the AC group than in the Ang II group ($P<0.001$; n=5; Fig. 1B). Similar trends for LVFS were demonstrated among all different groups (Fig. 1C). A higher LVFS was detected in the AC group ($P<0.001$) than in the Ang II group. Co-treatment with CKI decreased the LVDS values, compared with those of the Ang II group ($P<0.01$; Fig. 1D). However, there was no significant difference in LVDD between the two groups (Fig. 1E). These results indicated that the Ang II-treated mice exhibited a lower ejection force; however, co-treatment with CKI significantly improved the systolic function of the ventricle. Thus, CKI attenuated Ang II-mediated HF in mice.

CKI preserves myocardial injury biomarkers. The results presented in Fig. 2A and B confirmed that CKI significantly decreased the levels of myocardial injury biomarkers. The levels of cTn I were markedly increased in the Ang II group, compared with the control group ($P<0.001$; Fig. 2A). Co-treatment with CKI significantly reduced the levels of cTn I, compared with those of the Ang II group ($P<0.01$). The results also revealed that the mice exhibited lower NT-proBNP plasma levels in the AC group than in the Ang II group ($P<0.01$; Fig. 2B). The NT-proBNP levels were significantly reduced in the AC group, compared with those of the Ang II group ($P<0.01$). These results indicated that CKI reversed Ang II-induced myocardial damage.

CKI regulates myocardial structural damage. The ultrastructure of the myocardium in the left ventricle was observed using TEM (Fig. 2C). TEM images of the healthy control mice and CKI-treated mice demonstrated evenly scattered mitochondria throughout the myocardium, and these displayed a regular shape, with compact cristae, an intact membrane and orderly arrayed myocardial filaments with vivid Z lines. The Ang II-treated group exhibited cardiomyocyte edema, as well as multiple forms of damage to the cardiomyocyte membrane. The results of the present study also demonstrated irregularly arranged and severely ruptured myocardial filaments in the Ang II-treated group. In addition, the mitochondria exhibited diffuse swelling and differing sizes, with numerous vacuoles. Moreover, the cristae were ruptured, lysed and vacuolized. The mice co-treated with CKI exhibited heart mitochondria with no swelling, slightly damaged cristae, healthy myofibrils and orderly arranged myocardial filaments with vivid Z lines. The cardiomyocyte hypertrophy, edema and mitochondrial damage rates were markedly higher in the Ang II group than in the AC group.

CKI reduces apoptosis in heart tissue in vivo. The results of TUNEL assay demonstrated that continuous Ang II treatment significantly increased the number of TUNEL-positive cells (Fig. 3). Co-treatment with CKI decreased the number of TUNEL-positive cells in the AC group, and Ang II increased

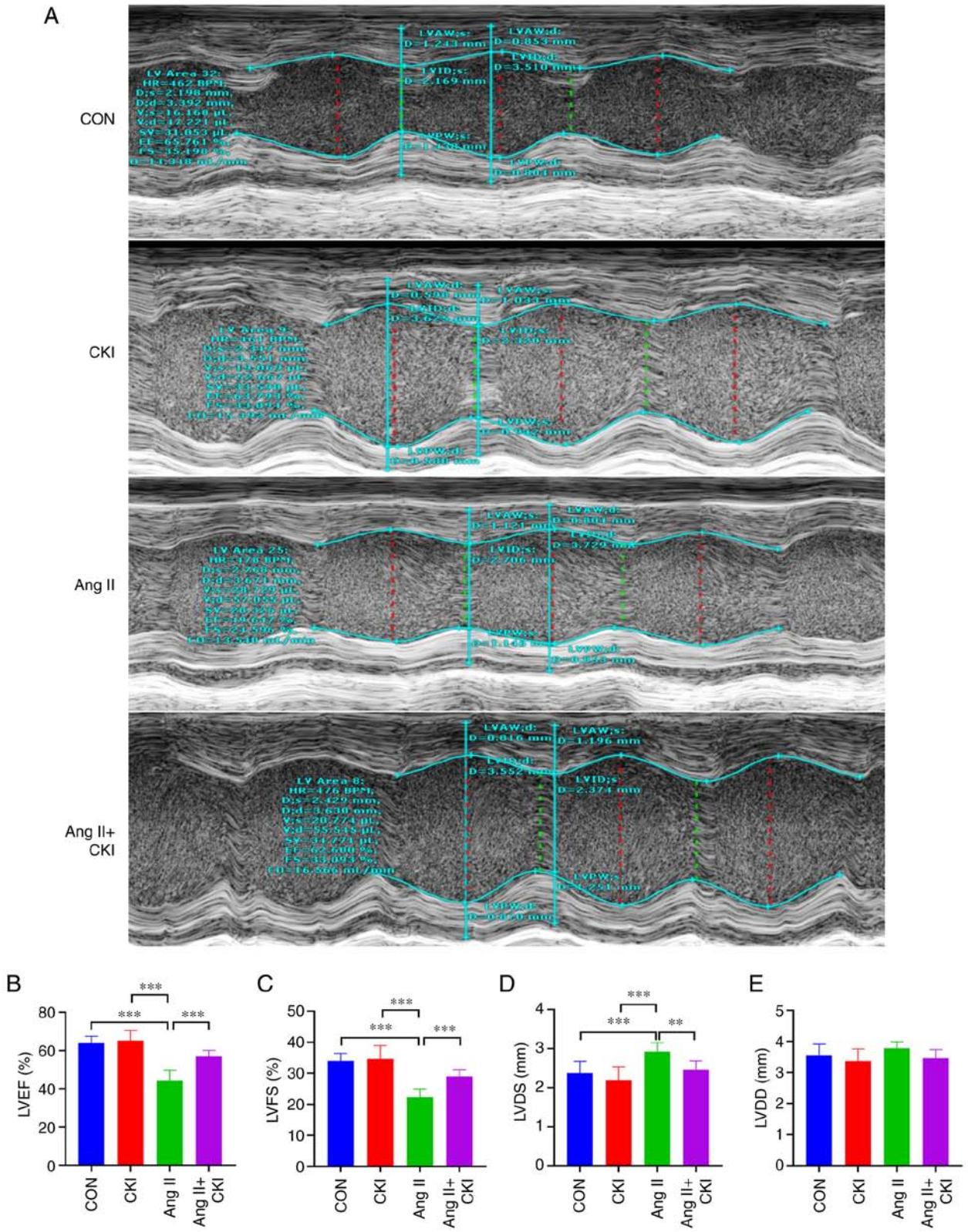

Figure 1. Doppler M-mode ultrasonography and markers of myocardial injury in serum. (A) Representative Doppler M-mode ultrasonography. (B) LVEF values in each group. (C) Similar trends were observed for LVFS among the different groups. (D) LVDS values, and (E) LVDD values. Data are presented as the mean ± SEM. One-way ANOVA and post-hoc Tukey's multiple comparisons test were used to determine statistically significant differences (n=10 mice per group). **P<0.01 and ***P<0.001. LVEF, left ventricular ejection fraction; LVDS, left ventricular end-systolic diameter; LVDD, left ventricular end-diastolic diameter; LVFS, left ventricular fraction shortening; CON, control; CKI, compound Kushen injection; Ang II, angiotensin II.

the apoptotic rate, compared with that in the AC group (P<0.001; Fig. 3). No notable trend was observed for the incidence of apoptosis in the CON or CKI groups, compared with the Ang II group (P<0.001; Fig. 3). Thus results of TUNEL assay thus revealed that CKI markedly reduced the apoptosis in the heart tissue.

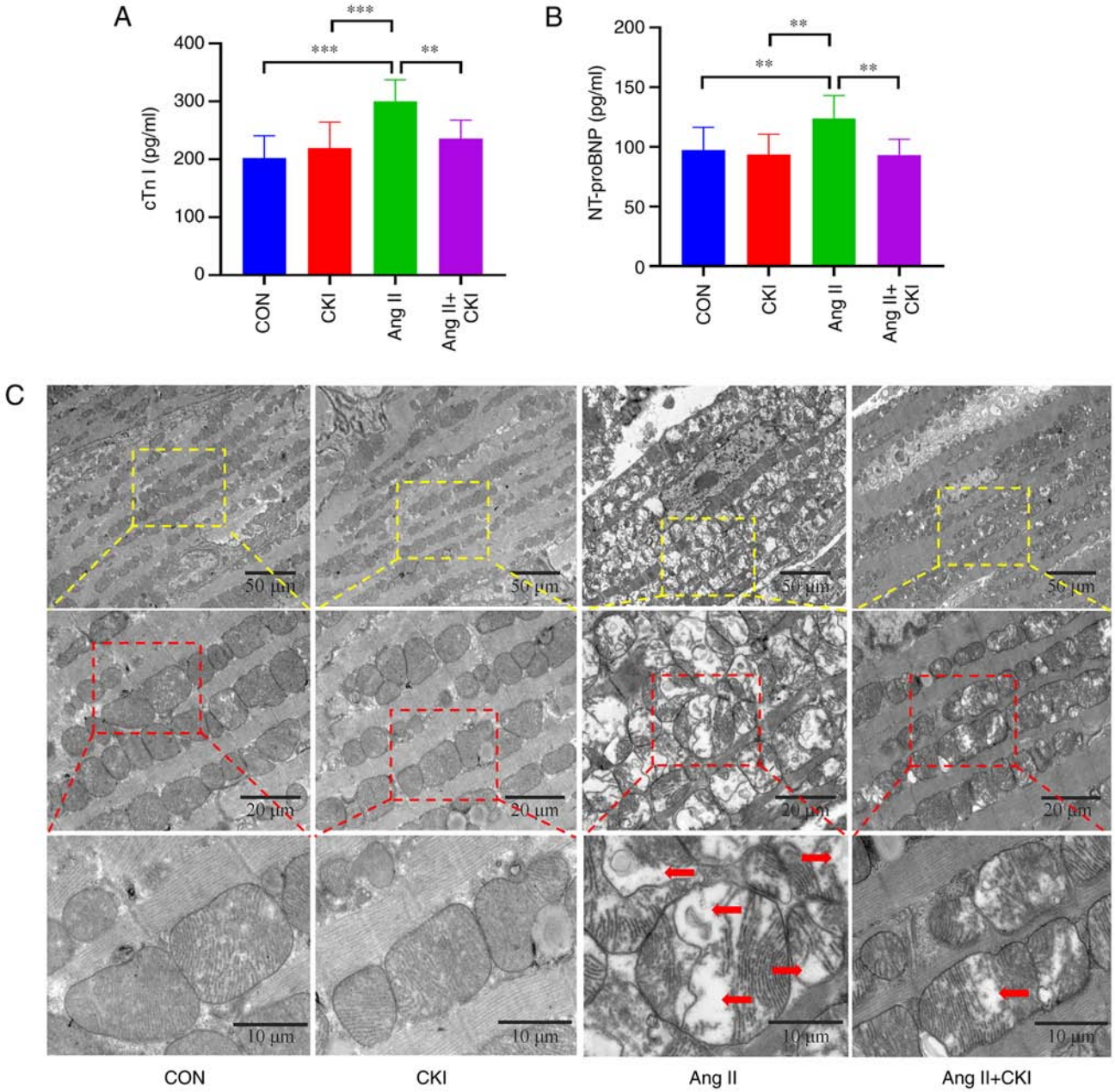

Figure 2. Myocardial injury biomarkers and morphometric analyses. The (A) cTn I level and (B) NT-proBNP level were detected in the different groups. (C) Transmission electron microscopy images of heart mitochondria and myocytes are shown. The arrows indicate vacuoles in the mitochondria. The images in the middle panel are the enlarged images of the area represented by the yellow boxes in the upper panel. The images on the bottom panel are the enlarged images of the areas represented by the red boxes in the middle panel. Scale bars: Upper panel, 50 μm; middle panel, 20 μm; bottom panel, 10 μm. Data are presented as the mean ± SEM. One-way ANOVA and post-hoc Tukey's multiple comparisons test were used to determine statistically significant differences (n=10 mice per group). **P<0.01 and ***P<0.001. cTn I, cardiac troponin I; NT-proBNP, N-terminal-pro hormone B-type natriuretic peptide; CON, control; CKI, compound Kushen injection; Ang II, angiotensin II.

FCM assay with Annexin V-PE/7-AAD double staining indicated that CKI inhibited cardiomyocyte apoptosis in the left ventricle (Fig. 4A). In the Ang II group, the population at the upper-right quadrant (Annexin V-PE$^+$/7-AAD$^+$), indicative of late apoptotic cells, was notably increased (4.284±1.071%), compared with that in the CON group (0.4±0.045%; P<0.001; Fig. 4B). In addition, the population at the lower-right quadrant (Annexin V-PE$^+$/7-AAD$^-$), indicative of early apoptotic cells, was significantly increased in the Ang II group (1.682±0.122%), compared with that in the CON group (0.61±0.082%; P<0.01, Fig. 4B). However, following co-treatment with CKI and Ang II, the population at the upper-right quadrant (0.64±0.122%) and lower-right quadrant (0.672±0.092%) was markedly decreased in the AC group, compared with the Ang II group. The total apoptotic rate, including early and late apoptosis, also decreased in the AC group (1.312±0.1%), compared with that of the Ang II group (5.966±1.038%; P<0.001; Fig. 4A). These findings revealed that CKI inhibited Ang II-mediated cardiomyocyte apoptosis.

The results of WB analysis (Fig. 5) demonstrated that Ang II notably increased the expression levels of PI3K, Bax, cyto *c*, cleaved caspase-9, cleaved caspase-9/total caspase-9, cleaved caspase-3 and cleaved caspase-3/total caspase 3 in the

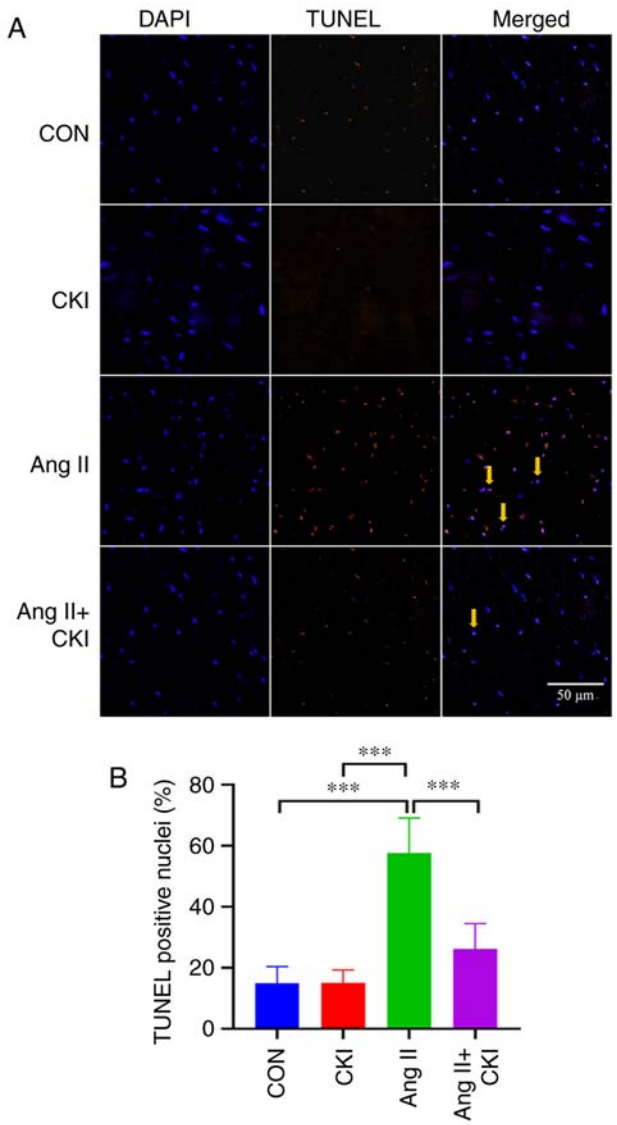

Figure 3. TUNEL assay and TUNEL-positive cell rate. (A) Representative TUNEL assay images of the different groups. The arrows indicate TUNEL-positive nuclei of cardiomyocytes. Scale bar, 50 μm. (B) The TUNEL-positive nuclei rate in the Ang II group. Data are presented as the mean ± SEM. One-way ANOVA and post-hoc Tukey's multiple comparisons test were used to determine statistically significant differences (n=5 mice per group). ***P<0.001. CON, control; CKI, compound Kushen injection; Ang II, angiotensin II.

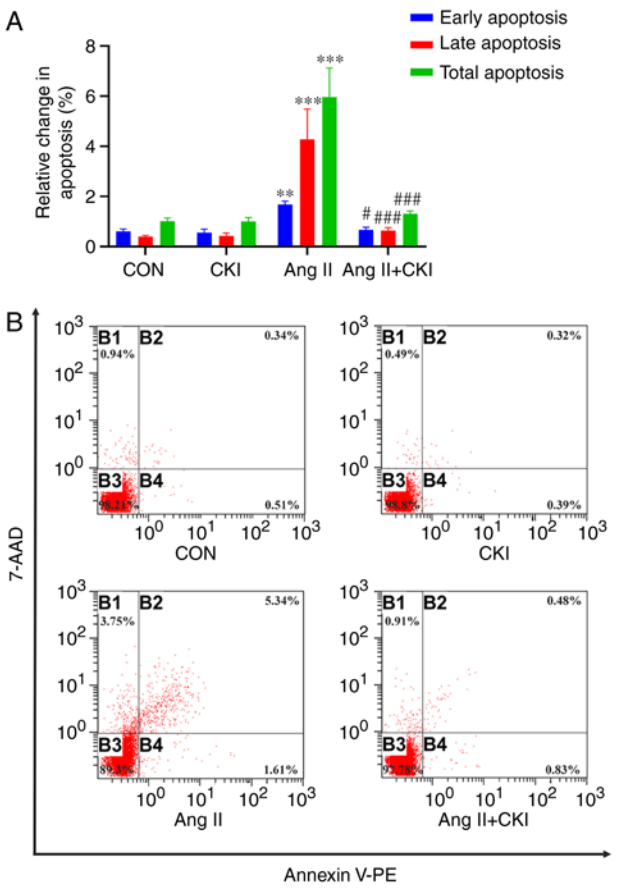

Figure 4. Flow cytometric assay with Annexin V-PE/7-AAD double staining and the apoptotic rate. (A) The early apoptotic rate, late apoptotic rate and total apoptotic rate are shown. (B) Flow cytometric assay with Annexin V-PE/7-AAD double staining in the different groups and the percentages in each quadrant. The quadrantes are as follows: B1, Annexin V-PE-/7-AAD+; B2, Annexin V-PE+/7-AAD+; B3, Annexin V-PE-/7-AAD-; B4, Annexin V-PE+/7-AAD-. Data are presented as the mean ± SEM. One-way ANOVA and post-hoc Tukey's multiple comparisons test were used to determine statistically significant differences (n=5 mice per group). **P<0.01 and ***P<0.001 vs. CON group; #P<0.05 and ###P<0.001 vs. Ang II group. CON, control; CKI, compound Kushen injection; Ang II, angiotensin II.

left ventricular tissue (Fig. 5B, G, H, I, K, L and N). In addition, Ang II notably decreased the expression levels of p-Akt, p-Akt/t-Akt and Bcl-2 (Fig. 5C, E and F). By contrast, CKI markedly increased the expression levels of p-Akt, p-Akt/t-Akt and Bcl-2 (Fig. 5C, E and F), and decreased the expression levels of PI3K, Bax, cyto *c*, cleaved caspase-9, cleaved caspase-9/total caspase-9, cleaved caspase-3 and cleaved caspase-3/total caspase-3 in the AC group (Fig. 5B, G, H, I, K, L and N). No significant differences were observed in the expression levels of t-Akt, total caspase-9 and total caspase-3 among the four groups (Fig. 5D, J and M).

CKI reduces the apoptosis of myocardial cells in vitro. The effects of CKI on the viability of the H9C2 cells were investigated using a CCK-8 assay. The results demonstrated that Ang II treatment significantly decreased H9C2 cell viability (P<0.001; Fig. 6A), and this decrease was reversed following treatment with CKI (P<0.05) and the PI3K/Akt pathway inhibitor, LY294002 (P<0.001) (Fig. 6A).

To examine whether CKI affects the cell cycle in myocardial cells, cell cycle distribution was investigated following treatment with CKI and LY294002, for 48 h. As shown in Fig. 6B and C, Ang II increased cell cycle arrest at the G_1 phase (P<0.01 vs. CON group) and decreased cell cycle arrest at the S phase in the H9C2 cells (P<0.01 vs. CON group). Following CKI treatment, the percentage of cells in the G_1 phase decreased (P<0.01 vs. Ang II group), and cell cycle arrest at the G_1 phase decreased. In addition, the percentage of cells at the S phase increased (P<0.01 vs. Ang II group). Similar trends were observed among the different phases in the AL group.

The results of WB analysis (Fig. 7) demonstrated that CKI significantly decreased the expression levels of PI3K, Bax and p27 in H9C2 cells (Fig. 7G, H and I). Moreover, the expression levels of p-Akt, Bcl-2 and cyclin D1, were significantly higher in the AC and AL groups, compared with the Ang II group

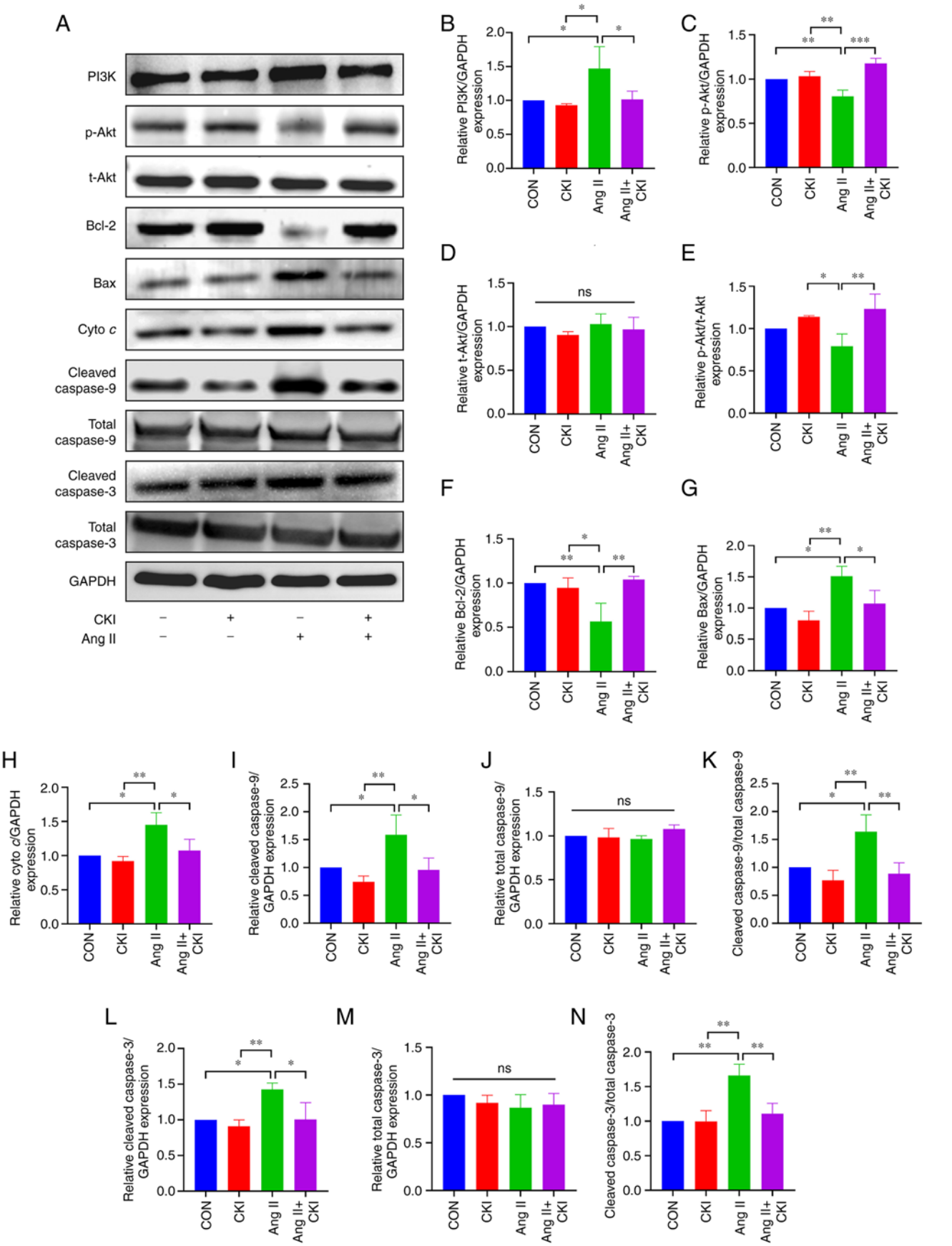

Figure 5. Expression of apoptosis-related proteins. (A) The results of western blot analysis for each protein. (B-N) The expression of representative proteins. (B) PI3K expression, (C) p-Akt expression, (D) t-Akt expression, (E) p-Akt/t-Akt ratio, (F) Bcl-2 expression, (G) Bax expression, (H) cyto c expression, (I) cleaved caspase-9 expression, (J) total caspase-9 expression, (K) cleaved caspase-9/total caspase-9, (L) cleaved caspase-3 expression, (M) total caspase-3 expression and (N) cleaved caspase-3/total caspase-3 in the different groups. Data are presented as the mean ± SEM. One-way ANOVA and post-hoc Tukey's multiple comparisons test were used to determine statistically significant differences (n=3 mice per group). *P<0.05, **P<0.01 and ***P<0.001. ns, not significant; CON, control; CKI, compound Kushen injection; Ang II, angiotensin II; cyto *c*, cytochrome *c*.

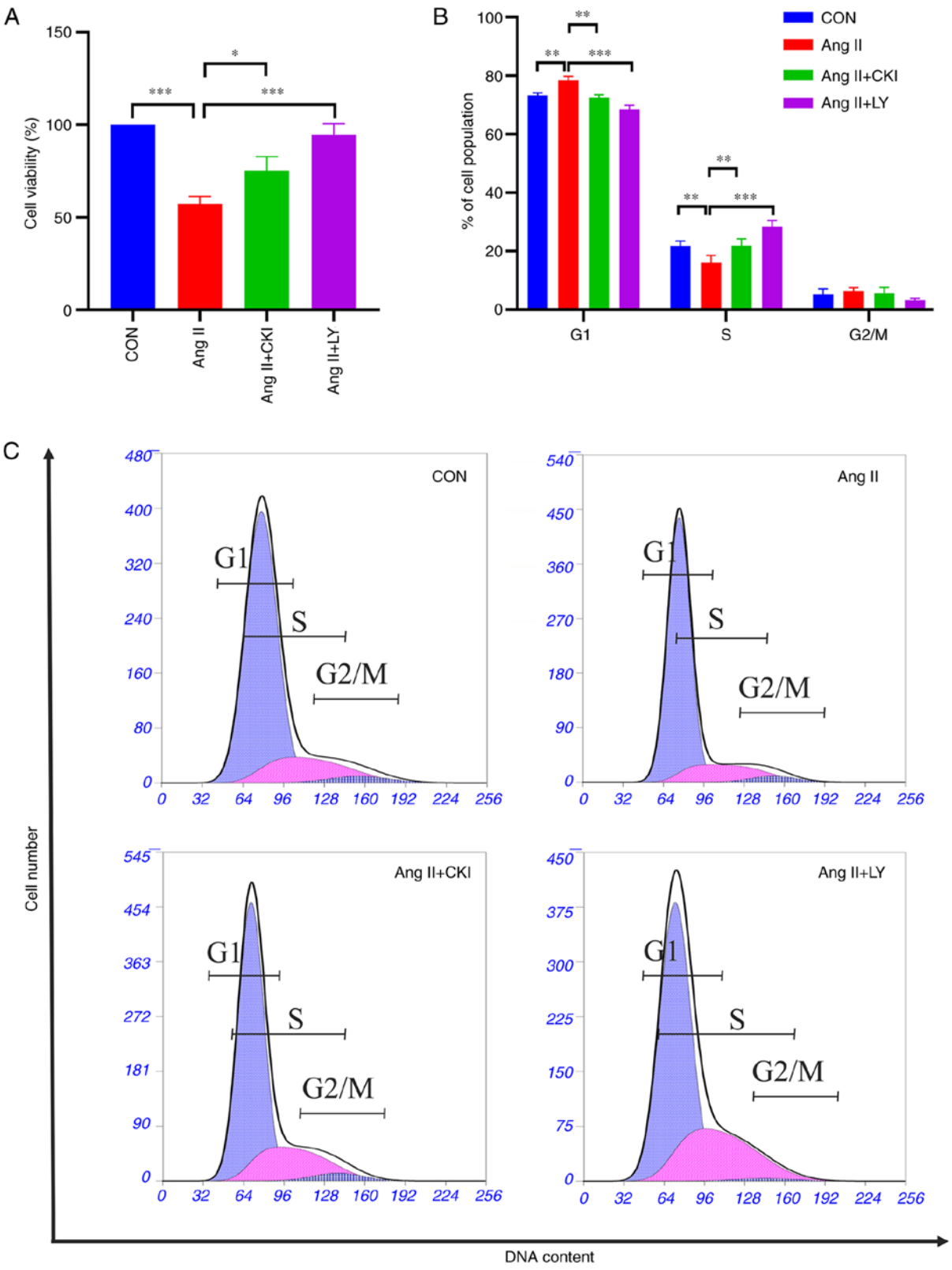

Figure 6. Cell proliferation *in vitro*. (A) CCK-8 assay for cell viability. (B) The cell cycle distribution rate. (C) Flow cytometry with PI staining represents the cell cycle distribution. Data are presented as the mean ± SEM. One-way ANOVA and post-hoc Tukey's multiple comparisons test were used to determine statistically significant differences (n=3 per group). *P<0.05, **P<0.01 and ***P<0.001. CON, control; CKI, compound Kushen injection; Ang II, angiotensin II; LY, LY294002 (an inhibitor of the PI3K/Akt pathway).

(Fig. 7B, E and F). A high p-Akt/t-Akt ratio was detected in the AC and AL groups (Fig. 7D). On the whole, these results demonstrated that CKI significantly reduced the expression of pro-apoptotic proteins in the H9C2 cells, and a similar trend was observed following treatment with the PI3K/Akt pathway inhibitor, LY294002.

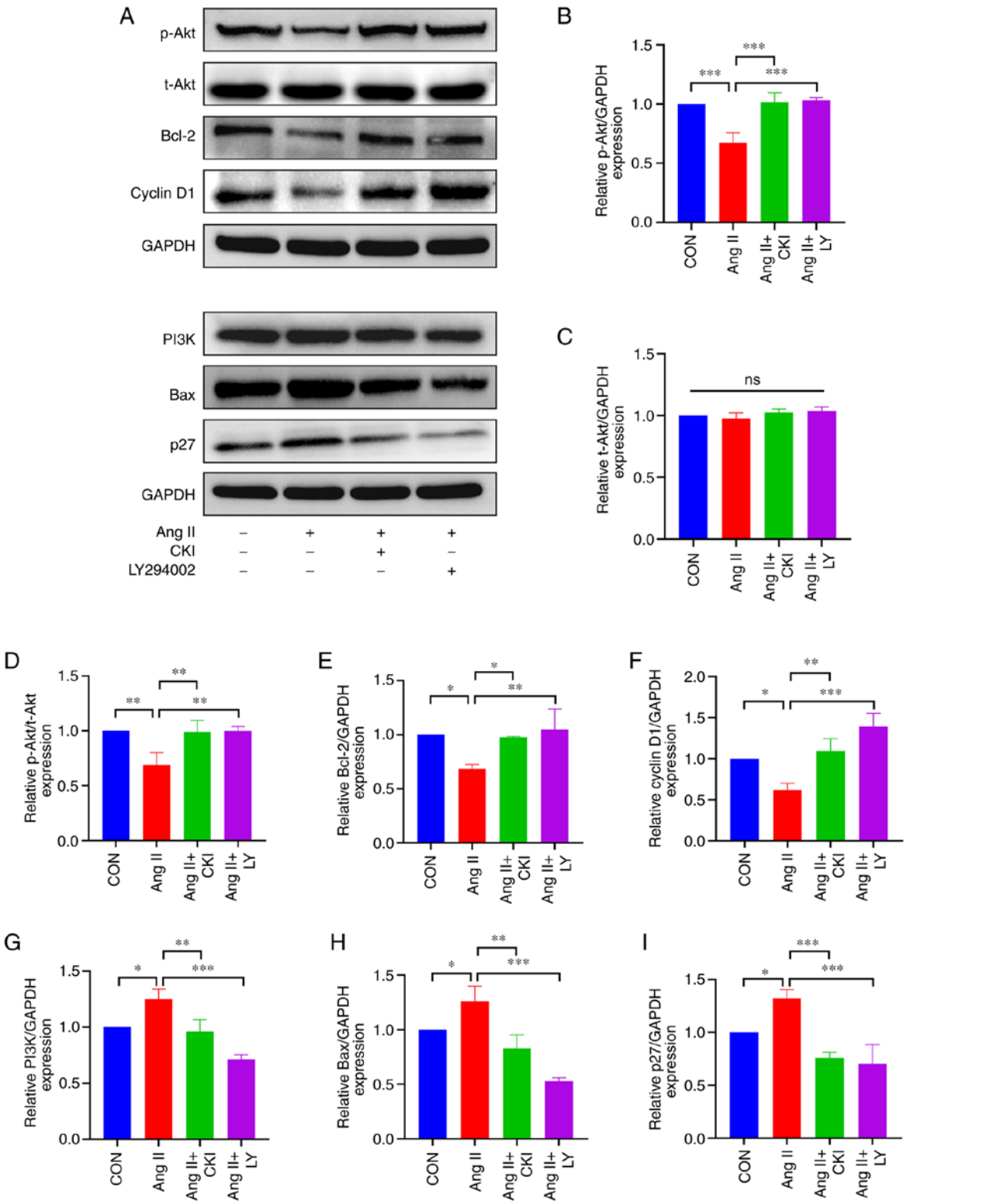

Figure 7. Expression of apoptosis-related proteins *in vitro*. (A) The results of western blot analysis for each protein. (B-I) The expression of representative proteins. (B) p-Akt expression, (C) t-Akt expression, (D) p-Akt/t-Akt ratio, (E) Bcl-2 expression, (F) cyclin D1 expression, (G) PI3K expression, (H) Bax expression, and (I) p27 expression in the different groups. Data are presented as the mean ± SEM. One-way ANOVA and post-hoc Tukey's multiple comparisons test were used to determine statistically significant differences (n=3 per group). *P<0.05, **P<0.01 and ***P<0.001. CON, control; CKI, compound Kushen injection; Ang II, angiotensin II; LY, LY294002 (an inhibitor of the PI3K/Akt pathway).

Discussion

HF is the final stage of numerous cardiac diseases. Inhibiting myocardial apoptosis may prevent cardiac remodeling and protect cardiac functions. To the best of our knowledge, the present study is the first to explore the association between the cardioprotective effects of CKI and the PI3K/Akt apoptotic pathway. CKI may promote healthy cardiac function, inhibit

heart structure remodeling and decrease cardiomyocyte apoptosis *in vivo* and *in vitro*. These effects were closely associated with the inactivation of pro-apoptotic proteins, such as PI3K, Bax, cyto *c*, cleaved caspase-9 and cleaved caspase-3, and the activation of apoptosis inhibitors, such as p-Akt and Bcl-2 in the PI3K/Akt pathway (Fig. 8). The results of the present study indicated that CKI may exert protective effects against HF.

Left ventricular enlargement and cardiac function decline may be early signs of HF. Notably, these factors may be associated with myocardial cell apoptosis, ventricular hypertrophy and cardiac structural remodeling. In the present study, the results of the M-mode ultrasonography demonstrated that the ventricular systolic and diastolic function were protected by CKI. cTnI is the gold standard biomarker for the detection of cardiac injury and myocardial cell necrosis (32). In addition, NT-proBNP is also used as a key biomarker to detect HF (33). In the present study, CKI significantly decreased cTnI and NT-proBNP. These results demonstrated that CKI protected the myocardium from damage.

The main pathological feature of HF is a decrease in cardiomyocytes caused by apoptosis, necrosis or myocardial fibrosis (34). The mitochondria are not only the main site of intracellular reactive oxygen species, but also the first target of myocardial function injury (35). Ang II promotes cardiomyocyte apoptosis, which is a main mechanism leading to HF (7). TEM images obtained in the present study demonstrated that Ang II elicited diffuse mitochondrial swelling, ruptured cristae and ruptured myocardial filaments. In addition, CKI treatment reduced mitochondrial apoptosis and promoted a regular structure. As the main site of myocardial cell death and survival, the mitochondria are of particular importance in the occurrence of HF. CKI may promote healthy cardiac function through reducing mitochondrial and cardiomyocyte apoptosis.

Apoptosis, as a type of programmed cell death, exerts a major effect on cell injury (36). In the present study, the apoptotic rates were analyzed using TUNEL and FCM assays. The results of TUNEL assay indicated that the Ang II group exhibited a markedly increased apoptotic rate. Following treatment with CKI, the number of apoptotic cardiomyocytes significantly decreased. In addition, the results of FCM assay demonstrated that CKI decreased the population of early and late apoptotic cells. The results of the TUNEL and FCM assays both confirmed that CKI reduced the apoptotic rate of cardiomyocytes.

To further determine whether the effects of CKI on HF are due to the inhibition of the PI3K/Akt pathway, the expression levels of representative signal proteins were determined using WB analysis. The PI3K/Akt apoptotic pathway is a key signaling pathway in HF (37). It plays a pro-apoptotic role by regulating the concentration of calcium, mitochondrial membrane stability and apoptotic gene expression (38). During myocardial injury, the PI3K/Akt signaling pathway is activated. Herein, CKI decreased the transcriptional activities of PI3K and Bax, and increased the expression of p-Akt and Bcl-2. As an apoptosis suppressor gene, Bcl-2 alleviates mitochondrial damage (39). An increased Bcl-2 expression inhibits apoptosis, which increases the stability of the mitochondrial membrane. The inhibition of the pro-apoptotic protein, Bax, may reduce mitochondrial damage (40). Cyto *c* is the main

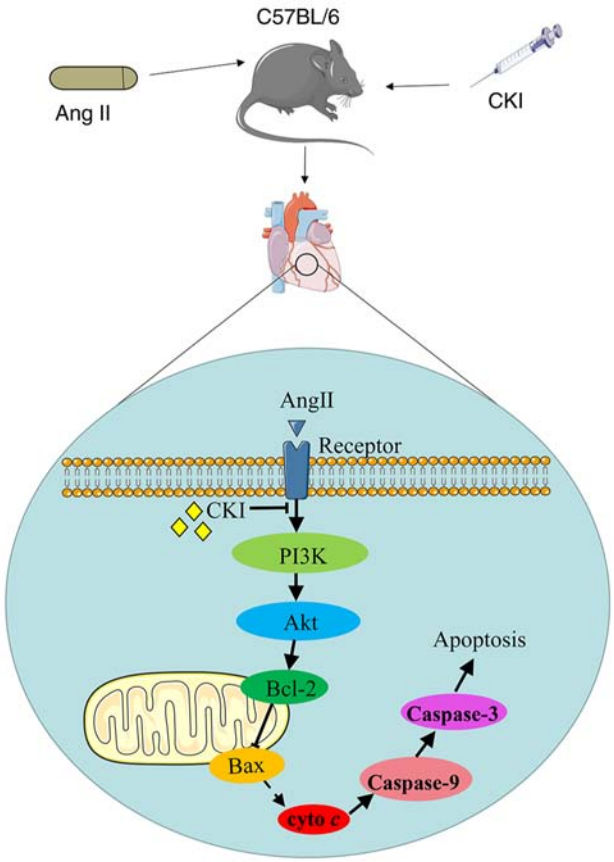

Figure 8. The mechanism through which CKI attenuates Ang II-mediated heart failure by inhibiting the PI3K/Akt pathway. C57BL/6 male mice were subcutaneously implanted with osmotic minipumps with Ang II. CKI was subcutaneously infused. CKI attenuated Ang II-mediated heart failure by inhibiting the PI3K/Akt apoptotic pathway. CKI, compound Kushen injection; Ang II, angiotensin II; cyto *c*, cytochrome *c*.

molecule released by mitochondria to promote cell apoptosis, which forms apoptosomes with Apoptotic protease activating factor-1 (APAF-1), ATP and caspase-9 precursor molecules in the cytoplasm (41). Apoptosomes trigger the activation of caspase-9 and increase cleaved caspase-9 expression, which activates caspase-3. Caspase-3 is a critical apoptosis-executing enzyme in the caspase family that plays a key role in various cell apoptotic pathways (42). When caspase-3 is activated, apoptosis occurs. The results of the present study demonstrated that Ang II activated the PI3K/Akt pathway and increased cleaved caspase-3 expression in myocardial cells. On the other hand, CKI inhibited the PI3K/Akt pathway and decreased cleaved caspase-3 expression. The persistence of cardiomyocyte apoptosis leads to a progressive cell loss in the myocardium, ventricle dilation and gradual cardiac remodeling, eventually leading to HF. In the present study, CKI alleviated myocyte injury and reduced cardiomyocyte apoptosis, thereby inhibiting HF. Collectively, these results indicate that the effects of CKI may be associated with the inactivation of pro-apoptotic mediators, such as PI3K, Bax, cyto *c*, cleaved caspase-9 and cleaved caspase-3, and the activation of apoptosis inhibitors, such as p-Akt and Bcl-2, in heart tissues.

To further determine the effects and potential underlying mechanisms, H9C2 cells were used to simulate an *in vitro* model of HF. In addition, the cells were treated with the

PI3K/Akt pathway inhibitor, LY294002. The results of CCK-8 assay demonstrated that CKI and LY294002 increased H9C2 cell viability, compared with the Ang II group. The cell cycle is a repeating series of events that occur in a cell, leading to cell division and DNA replication to produce two daughter cells (43). The cell cycle is divided into the interphase phase and metaphase phase (M). The cell interphase can be further divided into three phases, namely, the G_1 phase (period of time before mitosis and DNA replication), the S phase (period of DNA synthesis) and the G_2 phase (period between the S and M phase). Cells undergoing a temporary pause in cell division are in the G_0 phase. The disruption of the cell cycle inhibits cell growth and activates the process of apoptosis (44). The regulation of the cell cycle is usually dependent on G_1 phase arrest. The proliferation index (PI) is calculated using the following formula (45): $PI=(S + G_2/M)/(G_0/G_1 + S + G_2/M)$ x100%. As shown in Fig. 6C, the cells were accumulated in the G_1 phase in the Ang II group, while the percentage of cells in the S phase decreased. By contrast, the opposite results were observed following treatment with CKI and LY294002. Thus, the PI of the CKI and LY294002 group was higher than that in the Ang II group. These results indicate that CKI may promote myocardial cell proliferation and inhibit myocardial cell apoptosis.

The PI3K/Akt pathway plays a crucial role in regulating the cell cycle and cell apoptosis (18). Cell cycle progression is controlled by the cyclin-CDK complex and CDK inhibitor proteins. In the G_1/S checkpoint, cyclin D1 forms a complex with CDK4 and therefore inhibits pRb via phosphorylation, resulting in the release of E2F to promote progression through the G_1 phase (46). On the other hand, the activity of the CDK4-cyclin D1 complex is negatively controlled by CDK inhibitor proteins, such as p27. In the present study, the results of WB analysis indicated that Ang II-induced G^1 arrest may be attributed to the decreased expression of cyclin D1 and the increased expression of p27. Treatment with CKI increased the expression of cyclin D1 and decreased that of p27, similar to the effects of LY294002. Notably, the results of the *in vitro* analysis suggested that CKI inhibited the apoptosis of H9C2 cells, similar to the effects of the PI3K/Akt pathway inhibitor, LY294002.

CKI is a type of TCM formulation. The active compounds of CKI consist of matrine, oxymatrine, sophocarpine, sophoridine, sophorine and kurarinone. The cardioprotective function of CKI may be associated with the multiple components. As aforementioned, matrine has been shown to exhibit a number of therapeutic effects on the cardiovascular system. Matrine has been shown to improve the function of HF in mice by resisting the inflammatory response and oxidative stress, and decreasing cardiomyocyte apoptosis (47). Matrine suppresses cardiac fibrosis by inhibiting the TGF-β/Smad pathway in experimental diabetic cardiomyopathy (48). Furthermore, oxymatrine pre-treatment has been shown to protect cardiomyocytes from hypoxia/reoxygenation injury by modulating the PI3K/Akt pathway (26). Oxymatrine can attenuate HF by improving cardiac function and this amelioration is associated with the upregulation of sarcoplasmic/endoplasmic reticulum Ca^{2+} ATPase 2a and 6,7-dihydropteridine reductase (49). A series of previous studies demonstrated that sophocarpine exerted a number of protective effects on the heart, vessels and other tissues. Sophocarpine has been shown to reduce the myocardial infarct size and improve cardiac function follwing ischemia-reperfusion in rats via NF-κB inactivation (50). Sophocarpine potentially exerts antifibrotic effects on the heart by modulating the balance between pro-inflammatory cytokine expression and the collagen content level, as well as MMP expression via the NF-κB signaling pathway (51). In summary, different components protect cardiac functions via different pathways. In the present study, it was demonstrated that CKI, as a compound preparation, exerted cardioprotective effects by inhibiting the PI3K/Akt pathway.

The present study has certain limitations which should be mentioned. It remains unknown as to whether the cardiovascular protective effects of CKI are dependent on matrine or other compounds, and which compound or compounds are responsible for the cardioprotective effects. In addition, the present study only briefly referred to certain some previous studies (21-26,47-51) on matrine, oxymatrine and sophocarpine. There may be other components with beneficial cardioprotective effects. On the other hand, in the present study, it was indicated that CKI inhibited the PI3K/Akt pathway. This pathway may contribute to the effects of CKI, but may not be the primary target. To further demonstrate that the suppression of this pathway is the main mechanism of action of CKI, additional studies are warranted using transgenic animals or using the combination treatment of CKI and a PI3K/Akt pathway agonist. Due to the limited sample size, the authors were unable to adequately assess the most effective compound or pathway. Further research is thus required to verify which compound or pathway is primarily responsible for the cardioprotective effects. Moreover, although the results of the present study verified that CKI inhibited apoptosis, the percentage of TUNEL-positive cells observed following TUNEL staining was inconsistent with the apoptotic rate of cardiomyocytes determined by FCM. These results may differ due to different experimental techniques. Additional external validations and evaluations are required to verify the apoptotic rate.

In conclusion, to the best of our knowledge, the present study is the first to demonstrate that CKI attenuates Ang II-mediated HF *in vivo* and *in vitro*, and this amelioration is associated with the inhibition of the PI3K/Akt pathway. CKI markedly decreased the expression of pro-apoptotic proteins, including PI3K, Bax, cyto *c*, cleaved caspase-9 and cleaved caspase-3, while it significantly increased the expression of p-Akt and Bcl-2. In addition, CKI reduced cardiomyocyte apoptosis, decreased myocardial damage, prevented heart structure remodeling and promoted healthy cardiac function. Therefore, CKI may exhibit potential as a novel treatment option for promoting healthy cardiac function.

Acknowledgements

Not applicable.

Funding

The present study was supported by the Hebei Key Laboratory of Heart and Metabolism (grant no. SZX2021003), the China Hebei International Joint Research Center for Structural Heart Disease, the S&T Program of Hebei (grant nos. 203777117D

and 19277757D), and the Natural Science Foundation of Hebei Province (grant nos. H2021206399 and H2020206420).

Availability of data and materials

The datasets used and/or analyzed during the current study are available from the corresponding author on reasonable request.

Authors' contributions

WW and DL conceived and conducted the experiments. WW wrote the manuscript. LY and LC established the animal models. MM established the cell models. YL and YY performed the data curation. MW and GL supervised the experimental process and performed the statistical analysis. MZ and YA designed the research and provided funding acquisition. All authors confirm the authenticity of all the raw data. All authors have read and approved the final manuscript.

Ethics approval and consent to participate

All animal procedures were carried out in accordance with the Guide for the Care and Use of Laboratory Animals published by the US National Institutes of Health, and all animal experiments were approved by the Institutional Animal Care and Use Committee of The First Hospital of Hebei Medical University, Shijiazhuang, China (ethics approval no. 20220634).

Patient consent for publication

Not applicable.

Competing interests

The authors declare that they have no competing interests.

References

1. Pang H, Han B, Yu T and Zong Z: Effect of apelin on the cardiac hemodynamics in hypertensive rats with heart failure. Int J Mol Med 34: 756-764, 2014.
2. Mozaffarian D, Benjamin EJ, Go AS, Arnett DK, Blaha MJ, Cushman M, de Ferranti S, Després JP, Fullerton HJ, Howard VJ, *et al*: Heart disease and stroke statistics-2015 update: A report from the American heart association. Circulation 131: e29-e322, 2015.
3. Sinphitukkul K, Manotham K, Eiam-Ong S and Eiam-Ong S: Aldosterone nongenomically induces angiotensin II receptor dimerization in rat kidney: Role of mineralocorticoid receptor and NADPH oxidase. Arch Med Sci 15: 1589-1598, 2019.
4. Gao G, Chen W, Yan M, Liu J, Luo H, Wang C and Yang P: Rapamycin regulates the balance between cardiomyocyte apoptosis and autophagy in chronic heart failure by inhibiting mTOR signaling. Int J Mol Med 45: 195-209, 2020.
5. Kang PM and Izumo S: Apoptosis and heart failure: A critical review of the literature. Circ Res 86: 1107-1113, 2000.
6. Wan GX, Ji LH, Xia WB, Cheng L and Zhang YG: Bioinformatics identification of potential candidate blood indicators for doxorubicin-induced heart failure. Exp Ther Med 16: 2534-2544, 2018.
7. Tsutsumi Y, Matsubara H, Ohkubo N, Mori Y, Nozawa Y, Murasawa S, Kijima K, Maruyama K, Masaki H, Moriguchi Y, *et al*: Angiotensin II type 2 receptor is upregulated in human heart with interstitial fibrosis, and cardiac fibroblasts are the major cell type for its expression. Circ Res 83: 1035-1046, 1998.
8. Jurado Acosta A, Rysä J, Szabo Z, Moilanen AM, Serpi R and Ruskoaho H: Phosphorylation of GATA4 at serine 105 is required for left ventricular remodelling process in angiotensin II-induced hypertension in rats. Basic Clin Pharmacol 127: 178-195, 2020.
9. Fukami K, Ueda S, Yamagishi S, Kato S, Inagaki Y, Takeuchi M, Motomiya Y, Bucala R, Iida S,Tamaki K, *et al*: AGEs activate mesangial TGF-beta-Smad signaling via an angiotensin II type I receptor interaction. Kidney Int 66: 2137-2147, 2004.
10. Wang X, Meng H, Wang Q, Shao M, Lu W, Chen X, Jiang Y, Li C, Wang Y and Tu P: Baoyuan decoction ameliorates apoptosis via AT1-CARP signaling pathway in H9C2 cells and heart failure post-acute myocardial infarction rats. J Ethnopharmacol 252: 112536, 2020.
11. Zhan Y, Abe I, Nakagawa M, Ishii Y, Kira S, Miyoshi M, Oniki T, Kondo H, Teshima Y, Yufu K, *et al*: A traditional herbal medicine rikkunshito prevents angiotensin II-Induced atrial fibrosis and fibrillation. J Cardiol 76: 626-635, 2020.
12. Wang W, You RL, Qin WJ, Hai LN, Fang MJ, Huang GH, Kang RX, Li MH, Qiao YF, Li JW and Li AP: Anti-tumor activities of active ingredients in compound Kushen injection. Acta Pharmacol Sin 36: 676-679, 2015.
13. Wang HY, Hu HY, Rong H and Zhao XW: Effects of compound Kushen injection on pathology and angiogenesis of tumor tissues. Oncol Lett 17: 2278-2282, 2019.
14. Xu W, Lin H, Zhang Y, Chen X, Hua B, Hou W, Qi X, Pei Y, Zhu X, Zhao Z and Yang L: Compound Kushen injection suppresses human breast cancer stem-like cells by down-regulating the canonical Wnt/β-catenin pathway. J Exp Clin Canc Res 30: 103, 2011.
15. Lai BY, Chu AJ, Yu BW, Jia LY, Fan YY, Liu JP and Pei XH: Clinical effectiveness and safety of Chinese herbal medicine compound Kushen injection as an add-on treatment for breast cancer: A systematic review and meta-analysis. Evid Based Complement Alternat Med 2022: 8118408, 2022.
16. Zhao Z, Liao H and Ju Y: Effect of compound Kushen injection on T-cell subgroups and natural killer cells in patients with locally advanced non-small-cell lung cancer treated with concomitant radiochemotherapy. J Tradit Chin Med 36: 14-18, 2016.
17. Zhang J, Qu Z, Yao H, Sun L, Harata-Lee Y, Cui J, Aung TN, Liu X, You R, Wang W, *et al*: An effective drug sensitizing agent increases gefitinib treatment by down regulating PI3K/Akt/mTOR pathway and up regulating autophagy in non-small cell lung cancer. Biomed Pharmacother 118: 109169, 2019.
18. Wang R, Zhang Q, Peng X, Zhou C, Zhong YX, Chen X, Qiu Y, Jin M, Gong M and Kong D: Stellettin B induces G1 arrest, apoptosis and autophagy in human non-small cell lung cancer A549 cells via blocking PI3K/Akt/mTOR pathway. Sci Rep 6: 27071, 2016.
19. Liu MH, Zhang Y, He J, Tan TP, Wu SJ, Guo DM, He H, Peng J, Tang ZH and Jiang ZS: Hydrogen sulfide protects H9c2 cardiac cells against doxorubicin-induced cytotoxicity through the PI3K/Akt/FoxO3a pathway. Int J Mol Med 37: 1661-1668, 2016.
20. Ravingerová T, Matejíková J, Neckář J, Andelová E and Kolář F: Differential role of PI3K/Akt pathway in the infarct size limitation and antiarrhythmic protection in the rat heart. Mol Cell Biochem 297: 111-120, 2007.
21. Huang J and Xu H: Matrine: Bioactivities and structural modifications. Curr Top Med Chem 16: 3365-3378, 2016.
22. Xiao TT, Wang YY, Zhang Y, Bai CH and Shen XC: Similar to spironolactone, oxymatrine is protective in aldosterone-induced cardiomyocyte injury via inhibition of calpain and apoptosis-inducing factor signaling. PLoS One 9: e88856, 2014.
23. Zhou YH, Shan H, Qiao G, Sui X, Lu Y and Yang B: Inotropic effects and mechanisms of matrine, a main alkaloid from Sophora flavescens AIT. Biol Pharm Bull 31: 2057-2062, 2008.
24. Zhang S, Guo S, Gao XB, Liu A, Jiang W, Chen X, Yang P, Liu LN, Shi L and Zhang Y: Matrine attenuates high-fat diet-induced in vivo and ox-LDL-induced in vitro vascular injury by regulating the PKCα/eNOS and PI3K/Akt/eNOS pathways. J Cell Mol Med 23: 2731-2743, 2019.
25. Li Y, Wang B, Zhou C and Bi Y: Matrine induces apoptosis in angiotensin II-stimulated hyperplasia of cardiac fibroblasts: Effects on Bcl-2/Bax expression and caspase-3 activation. Basic Clin Pharmacol Toxicol 101: 1-8, 2007.
26. Zhang Z, Qin X, Wang Z, Li Y, Chen F, Chen R, Li C, Zhang W and Zhang M: Oxymatrine pretreatment protects H9c2 cardiomyocytes from hypoxia/reoxygenation injury by modulating the PI3K/Akt pathway. Exp Ther Med 21: 556, 2021.
27. National Research Council of The National Academies: Guide for the care and use of laboratory animals. Eighth edition. The National Academies Press, Washington, DC, 2011.

28. Liu D, Zhan Y, Ono K, Yin Y, Wang L, Wei M, Ji L, Liu M, Liu G, Zhou X and Zheng M: Pharmacological activation of estrogenic receptor G protein-coupled receptor 30 attenuates angiotensin II-induced atrial fibrosis in ovariectomized mice by modulating TGF-β1/smad pathway. Mol Biol Rep 49: 6341-6355, 2022.
29. Zhao Z, Fan H, Higgins T, Qi J, Haines D, Trivett A, Oppenheim JJ, Wei H, Li J, Lin H and Howard OM: Fufang Kushen injection inhibits sarcoma growth and tumor-induced hyperalgesia via TRPV1 signaling pathways. Cancer Lett 355: 232-241, 2014.
30. Qu Z, Cui J, Harata-Lee Y, Aung TN, Feng Q, Raison JM, Kortschak RD and Adelson DL: Identification of candidate anti-cancer molecular mechanisms of compound Kushen injection using functional genomics. Oncotarget 7: 66003, 2016.
31. Chen S, Liu J, Liu X, Fu Y, Zhang M, Lin Q, Zhu J, Mai L, Shan Z, Yu X, *et al*: Panax notoginseng saponins inhibit ischemia-induced apoptosis by activating PI3K/Akt pathway in cardiomyocytes. J Ethnopharmacol 137: 263-270, 2011.
32. Omland T, de Lemos JA, Sabatine MS, Christophi CA, Rice MM, Jablonski KA, Tjora S, Domanski MJ, Gersh BJ, Rouleau JL, *et al*: A sensitive cardiac troponin T assay in stable coronary artery disease. N Engl J Med 361: 2538-2547, 2009.
33. Vergaro G, Gentile F, Meems LMG, Aimo A, Januzzi JL Jr, Richards AM, Lam CSP, Latini R, Staszewsky L, Anand IS, *et al*: NT-proBNP for risk prediction in heart failure: Identification of optimal cutoffs across body mass index categories. JACC Heart Fail 9: 653-663, 2021.
34. Tham YK, Bernardo BC, Ooi JYY, Weeks KL and McMullen JR: Pathophysiology of cardiac hypertrophy and heart failure: Signaling pathways and novel therapeutic targets. Arch Toxicol 89: 1401-1438, 2015.
35. Goldenthal MJ: Mitochondrial involvement in myocyte death and heart failure. Heart Fail Rev 21: 137-155, 2016.
36. Yao L, Chen H, Wu Q and Xie K: Hydrogen-rich saline alleviates inflammation and apoptosis in myocardial I/R injury via PINK-mediated autophagy. Int J Mol Med 44: 1048-1062, 2019.
37. Sarbassov DD, Guertin DA, Ali SM and Sabatini DM: Phosphorylation and regulation of Akt/PKB by the rictor-mTOR complex. Science 307: 1098-1101, 2005.
38. Zhou Z, Zhang Y, Lin L and Zhou J: Apigenin suppresses the apoptosis of H9C2 rat cardiomyocytes subjected to myocardial ischemia-reperfusion injury via upregulation of the PI3K/Akt pathway. Mol Med Rep 18: 1560-1570, 2018.
39. Siddiqui WA, Ahad A and Ahsan H: The mystery of BCL2 family: Bcl-2 proteins and apoptosis: An update. Arch Toxicol 89: 289-317, 2015.
40. Er E, Oliver L, Cartron PF, Juin P, Manon S and Vallette FM: Mitochondria as the target of the pro-apoptotic protein Bax. Biochim Biophys Acta 1757: 1301-1311, 2006.
41. Riedl SJ and Salvesen GS: The apoptosome: Signalling platform of cell death. Nat Rev Mol Cell Bio 8: 405-413, 2007.
42. Jeong SY, Han MH, Jin CY, Kim GY, Choi BT, Nam TJ, Kim SK and Choi YH: Apoptosis induction of human leukemia cells by Streptomyces sp. SY-103 metabolites through activation of caspase-3 and inactivation of Akt. Int J Mol Med 25: 31-40, 2010.
43. Qin J, Tao D, Duan R, Leng Y, Shen M, Zhou H, Feng Y, Gao C, Yu Y, Li QQ, *et al*: Cytokinetic analysis of cell cycle and sub-phases in MOLT-4 cells by cyclin E + A/DNA multiparameter flow cytometry. Oncol Rep 9: 1041-1045, 2002.
44. Meikrantz W and Schlegel R: Apoptosis and the cell cycle. J Cell Biochem 58: 160-174, 1995.
45. Zhao Y, Chen Y, Wang J and Liu L: Effects of ATP-binding cassette transporter G2 in extracellular vesicles on drug resistance of laryngeal cancer cells in *in vivo* and *in vitro*. Oncol Lett 21: 364, 2021.
46. Lukas J, Bartkova J, Rohde M, Strauss M and Bartek J: Cyclin D1 is dispensable for G1 control in retinoblastoma gene-deficient cells independently of cdk4 activity. Mol Cell Biol 15: 2600-2611, 1995.
47. Liu Y, Lian Q, Li X, Zhou X, Gao H and Cui T: Matrine alleviates heart failure in rats by resisting inflammatory response and oxidative stress and reducing cardiac myocyte apoptosis. Lat Am J Pharm 38: 2170-2176, 2019.
48. Zhang Y, Cui L, Guan G, Wang J, Qiu C, Yang T, Guo Y and Liu Z: Matrine suppresses cardiac fibrosis by inhibiting the TGF-β/Smad pathway in experimental diabetic cardiomyopathy. Mol Med Rep 17: 1775-1781, 2018.
49. Hu ST, Tang Y, Shen YF, Ao HH, Bai J, Wang YL and Yang YJ: Protective effect of oxymatrine on chronic rat heart failure. J Physiol Sci 61: 363-372, 2011.
50. Li C, Gao Y, Tian J, Shen J, Xing Y and Liu Z: Sophocarpine administration preserves myocardial function from ischemia-reperfusion in rats via NF-κB inactivation. J Ethnopharmacol 135: 620-625, 2011.
51. Li J, Li L, Chu H, Sun X and Ge Z: Oral sophocarpine protects rat heart against pressure overload-induced cardiac fibrosis. Pharm Biol 52: 1045-1051, 2014.